

ENHANCEMENT OF MPPT MODULE FOR PARTIAL SHADING PHOTOVOLTAIC SYSTEM UNDER UNIFORM IRRADIANCE CONDITIONS

HAMEED ALI MOHAMMED¹, ROSMIWATI MOHD-MOKHTAR^{1*}
AND HAZEM IBRAHIM ALI²

¹*School of Electrical and Electronic Engineering, University Sains Malaysia, Nibong Tebal, Pulau Pinang, Malaysia*
²*Control and Systems Engineering Department, University of Technology-Iraq, Baghdad, Iraq*

*Corresponding author: eerosmiwati@usm.my

(Received: 17 February 2023; Accepted: 15 April 2023; Published online: 4 July 2023)

ABSTRACT: Maximum Power Point Tracking (MPPT) algorithms play a critical role in maximizing the output power of solar panels. Different MPPT techniques are evaluated based on several criteria, such as tracking speed, simplicity, and accuracy with changes in solar irradiance and ambient temperature. Under partial shading conditions (PSCs), conventional techniques fail to track global maximum power points (GMPP). This paper aims to present an automatic and accurate method to fix the complexity of determining the accurate lookup table data in an automatic and fast process under uniform irradiance conditions (UICs) and PSCs. The proposed method runs the photovoltaic (PV) module with all potential irradiance and temperature. It automatically calculates the perfect voltage reference (V_{ref}) for all potential PV system cases. The V_{ref} is collected in an array, sent into a two-dimensional lookup table, and used for controlling the boost converter. Simulation results verify the effectiveness of the proposed method. In addition, a comparison was also made with the conventional perturb and observe (P&O) method. Under UICs, the proposed method takes less time than the conventional P&O algorithm to reach the MPP. The time difference between them is $\Delta t = 0.133$ sec and $\Delta t = 0.04$ sec for the first scanning process at $t = 0$ sec and sudden change irradiance at $t = 1.5$ sec, respectively. As for PSCs, the proposed method reached the GMPP during pattern 104 (first peak) without any power loss, while the P&O MPPT was able to track the GMPP but with power losses of 2729.97 watts.

ABSTRAK: Algoritma Penjejakan Titik Kuasa Maksimum (MPPT) memainkan peranan penting dalam memaksimumkan kuasa keluaran panel solar. Teknik MPPT yang berbeza dinilai berdasarkan beberapa kriteria seperti kelajuan pengesanan, kesederhanaan, dan ketepatan dengan perubahan dalam sinaran suria dan suhu ambien. Di bawah keadaan teduhan separa (PSC), teknik konvensional gagal menjejak titik kuasa maksimum global (GMPP). Kajian ini bertujuan bagi membentangkan kaedah automatik dan tepat bagi membetulkan kesusahan dalam menentukan carian data berjadual secara tepat, automatik dan pantas di bawah keadaan sinaran seragam (UIC) dan PSC. Kaedah yang dicadangkan menjalankan modul fotovoltai (PV) dengan semua potensi sinaran dan suhu dan mengira rujukan voltan sempurna (V_{ref}) secara automatik bagi semua kes yang berpotensi dalam sebarang jenis sistem PV. V_{ref} dikumpul dalam tata susunan, dihantar ke dalam jadual carian dua dimensi, dan digunakan bagi mengawal penukar rangsangan. Keputusan simulasi mengesahkan keberkesanan kaedah yang dicadangkan. Perbandingan juga dibuat dengan kaedah konvensional perhati dan ganggu (P&O). Di bawah UIC, kaedah yang dicadangkan mengambil masa yang lebih singkat berbanding algoritma konvensional P&O bagi mencapai MPP. Perbezaan masa antara keduanya adalah masing-masing, $\Delta t =$

0.133 saat dan $\Delta t = 0.04$ saat bagi proses pengimbasan pertama iaitu pada $t = 0$ saat dan sinaran perubahan mendadak pada $t = 1.5$ saat. Bagi PSC, kaedah yang dicadangkan mencapai GMPP semasa corak 104 (puncak pertama) tanpa kehilangan kuasa manakala MPPT P&O dapat mengesan GMPP tetapi dengan pengurangan kuasa sebanyak 2729.97 watt.

KEYWORDS: *photovoltaic; global maximum power point; maximum power point tracking; lookup table method; partial shading condition*

1. INTRODUCTION

The MPPT is a critical technique for getting maximum power from a PV panel system. The electrical energy is obtained directly from a group of connected PV cells. Solar irradiance and ambient temperature conditions affect the amount of extracted power from the PV module. The MPPT technique aims to dynamically obtain the maximum power by forcing the PV panel to work at an efficient voltage operating point (VMPP) [1,2]. The MPPT technique can be classified into two methods, under UICs and PSCs. In the UICs case, classical MPPT techniques include constant perturb and observe (P&O), incremental conductance (InC), open-circuit voltage (OCV), short circuit current (SCC), lookup table, and hill-climbing (HC) methods [3]. The nonlinearity of the P-V curve for the PV system means it only has one optimum operating point called the maximum power point (MPP). The location of this point on the P-V curve significantly depends on atmospheric conditions, such as irradiance and ambient temperature. During PSCs, the P-V curve will have several local maximum power points (LMPPs) and only one global maximum power point (GMPP) [4,5]. The aforementioned techniques are sometimes combined with other methods to find the GMPP.

Conventional MPPT techniques suffer from three major drawbacks; 1) rapid oscillations around the MPP even at the steady-state response, 2) the inability to effectively track during sudden changes in irradiance, and 3) the inability to identify the GMPP during PSCs because they may be busy in one of the LMPPs. This situation creates a complicated process to find the system's GMPP [6,7]. Research has been done in the literature to overcome the drawbacks of conventional MPPT techniques. A two-phased tracking method was presented to improve the tracking behavior of the conventional incremental conductance MPPT [8]. The method improved the performance of the conventional InC MPPT, but it was still unable to track the GMPP during PSCs.

Research by Basoglu used the concept of the OCV method to first estimate the locations of GMPP by assuming that the maximum power point was located at 0.85 and 0.8 of open-circuit voltage, respectively [9]. Then, the P&O MPPT algorithm was used to track the maximum point. The method has a good tracking performance, but it is ineffective when the peaks are not always in ascending order toward the GMPP. An optimization method called artificial bee colony (ABC) was presented in [10]. The drawbacks of this algorithm are slow tracking, and even though the technique can track under PSCs with high tracking speed, the efficiency declines when the shading patterns are changed immediately.

Also, the general drawbacks of the method were the implementation complexity, and the high financial cost. The method presented in [11] estimated the MPP by calculating the I-V curve's maximum power point voltage (VMPP). Regrettably, the method resulted in lower output power than the P&O technique. Also, the method was unable to find the GMPP under PSCs. In [12], adaptive neuro-fuzzy inference system (ANFIS) MPPT techniques were trained for the non-linear characteristic of the PV system. These algorithms had a high

accuracy under rapid changes in irradiance conditions. However, they had a high complexity in selecting the output target data and could not be implemented quickly. Authors in [13] and [14] used the Lookup Table technique and compared it with P&O MPPT.

This technique's problem was the complexity of calculating the lookup table data, especially under PSCs. Moreover, the lookup table data must be increased to get highly accurate tracking and cover all operating points, thus increasing the calculation difficulties. To solve the complexity problem, the authors in [15] and [16] combined P&O MPPT and Lookup Table MPPT. The method recorded the irradiance and duty cycle values from the P&O MPPT and sent the data into a table to use the next time. The method could not enhance the performance of P&O MPPT because it used the same duty cycle used in the P&O method, which limited this method with the P&O algorithm limitation.

For designing lookup table systems, the researchers faced a big problem with determining the table data accurately. The design process needed a large amount of accurate data to ensure accurate results. Moreover, MPPT based on the lookup table method was inefficient under PSCs. This paper proposes an automatic and accurate method to solve the problem of the calculation complexity associated with the lookup table method and makes it capable of tracking the GMPP and working efficiently under PSCs. This method can calculate and track the MPP for any PV system under UICs and PSCs and builds a complete data array that contains PMPP and corresponding voltage VMPP for all potential cases in just a few minutes.

2. SOLAR ARRAY MATHEMATICAL MODEL

The single-diode PV array equivalent circuit is shown in Fig. 1. The current source (I_{ph}) represents the cell photocurrent connected in parallel with a diode. N_s is the number of series cells, N_p is the number of parallel cells, R_{sh} and R_s are the shunt and series resistances of the cell, respectively [15,16]. The current source (I_{ph}) is described by [17]

$$I_{ph} = I_{sc} + K_i(T - 298) \cdot G/1000 \quad (1)$$

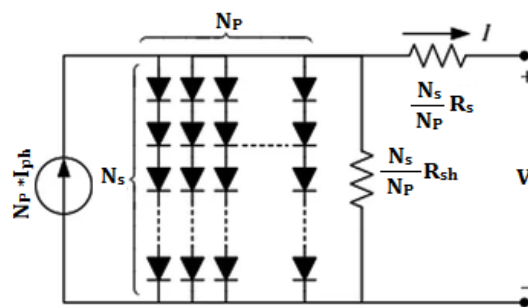


Fig. 1: Equivalent circuit of solar array [17].

where I_{sc} is the short-circuit current (A), K_i is the short-circuit current of the cell at 25 °C and 1000 W/m², T is the operating temperature (K), and G is the solar irradiation (W/m²). The reverse saturation current (I_{rs}) is

$$I_{rs} = I_{sc} / [\exp(q \cdot V_{OC} / N_s \cdot k \cdot n \cdot T) - 1] \quad (2)$$

where q is the electron charge (1.6×10^{-19}), V_{OC} is the open-circuit voltage (V), n is the ideality factor of the diode, and k is the Boltzmann's constant (1.3805×10^{-23} J/K). The saturation current (I_0) is given by

$$I_0 = I_{rs}(T/T_r)^3 \exp\left[\left(q \cdot E_{g0}/n \cdot k\right)(1/T_r - 1/T)\right] \quad (3)$$

where T_r is the nominal temperature (298 K), E_{g0} is the bandgap energy of the semiconductor (1.1 eV). The PV module output current (I) is [15]

$$I = I_{ph}N_p - I_0N_s \left[\exp\left(\left((V/N)s + (I \cdot R_s/N_p)/n \cdot v_t\right)\right) - 1 \right] - I_{sh} \quad (4)$$

with

$$v_t = k \cdot T/q \quad (5)$$

$$I_{sh} = (V(N_p/N_s) + I \cdot R_s)/R_{sh} \quad (6)$$

where v_t is the diode thermal voltage (V), and I_{sh} is the current through the shunt resistance. This paper uses ERA Solar ESPMC-215 PV Model as a reference module. The PV model parameters are given in Table 1.

Table 1: Parameters of ESPMC-215 PV module

| Name | Symbol | Value |
|---------------------------------------|-----------|----------|
| Maximum power | P_{MPP} | 213.15 W |
| Voltage at the maximum power point | V_{MPP} | 29.00 V |
| Current at the maximum power point | I_{MPP} | 7.350 A |
| Open circuit voltage | V_{oc} | 36.30 V |
| Short circuit current | I_{sc} | 7.840 A |
| Number of cells connected in series | N_s | 10 |
| Number of cells connected in parallel | N_p | 40 |

3. PROPOSED METHOD

The P&O MPPT algorithm is the most well-known technique because of its ease of design and implementation. From the flowchart shown in Fig. 2, notice that the P&O MPPT determinations compare the change in PV power, ΔP , and change in PV voltage, ΔV , for two points, K and $K-1$, on a P-V curve to identify the maximum power point. The main disadvantages of this technique are inability to deal with rapid weather changes, high oscillations around the MPP, the slow response, and failure to track GMPP under PSC [18], [19].

To avoid the disadvantages of the P&O MPPT method and solve the complexity problem associated with the lookup table method and make it work efficiently under PSCs, an automatic and accurate method is proposed in this paper. In the first step, the method starts to ask the user to enter the specifications of the solar array, the maximum and minimum limits of solar radiation (G_{MAX} and G_{MIN}), and the maximum and minimum limits of the ambient temperature (T_{MAX} and T_{MIN}) respectively, as well as the number of connected cells in series (N_s) and parallel (N_p). The flowchart in Fig. 3 shows the whole tracking process of the proposed method.

Then, it runs the PV module and measures the PV voltage (V_{PV}) and current (I_{PV}) and calculates the PV power (P_{PV}). From the V_{PV} and P_{PV} that have been calculated, it generates the PV curves for all operating point cases (for all potential irradiance and temperatures). It calculates the MPP for each operating point case. After calculating MPPs, it automatically calculates the corresponding voltage for every MPP without manual calculation and considers it a reference voltage (V_{ref}). After finishing all offline testing cases, it collects all the calculated reference voltages in an array and sends them with input vectors (irradiance and temperature) into a lookup table. The lookup table makes the V_{ref} array more flexible because it uses this array to map input values to output values, allowing the system to estimate the missing data. The system has been divided into three groups of PV modules connected in series to simulate the PSCs. Group 1 is set as no shading PV array, while Groups 2 and 3 are shading PV arrays with 20 shading patterns for each. The details are explained in the next section.

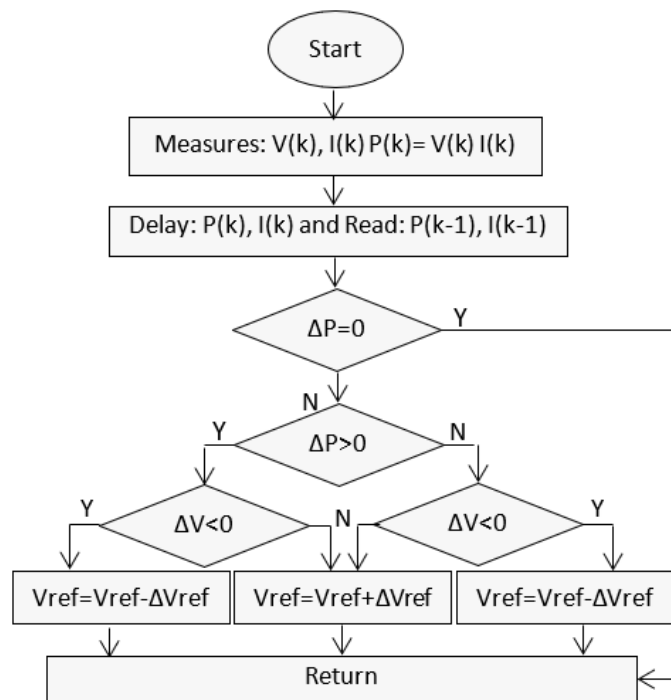


Fig. 2: Flowchart of P&O algorithm.

The proposed method is evaluated for 400 patterns (20x20) and calculates the GMPP for each pattern. It calculates the MPP irrespective of the number of peaks on the PV curve, which allows this method to work effectively under PSCs. This capability is considered one of the most vital points of the proposed method.

In this paper, a boost converter is designed and used as a power driver between the PV array and the load to adjust the solar module voltage to extract the maximum power from the PV array at the converter input side. The system uses the V_{ref} generated from the proposed MPPT method and compares it with the actual V_{PV} to generate an error signal. The Proportional Integral (PI) controller has been designed to manage the error signal and generate the duty ratio to control the boost converter. On the other hand, the parameters of the boost converter, as given in Table 2, have been calculated carefully to achieve minimum fluctuation around the MPP. Figure 4 shows the overall system, PV array, MPP method, boost converter, and PI controller.

Table 2: Parameters of a boost converter

| Name | Symbol | Value |
|-------------------|-----------|--------------|
| Input capacitor | C_{in} | 3227 μ F |
| Inductor | L | 1.45 mH |
| Output capacitor | C_{out} | 1000 μ F |
| Output resistance | R_{OUT} | 20 Ω |

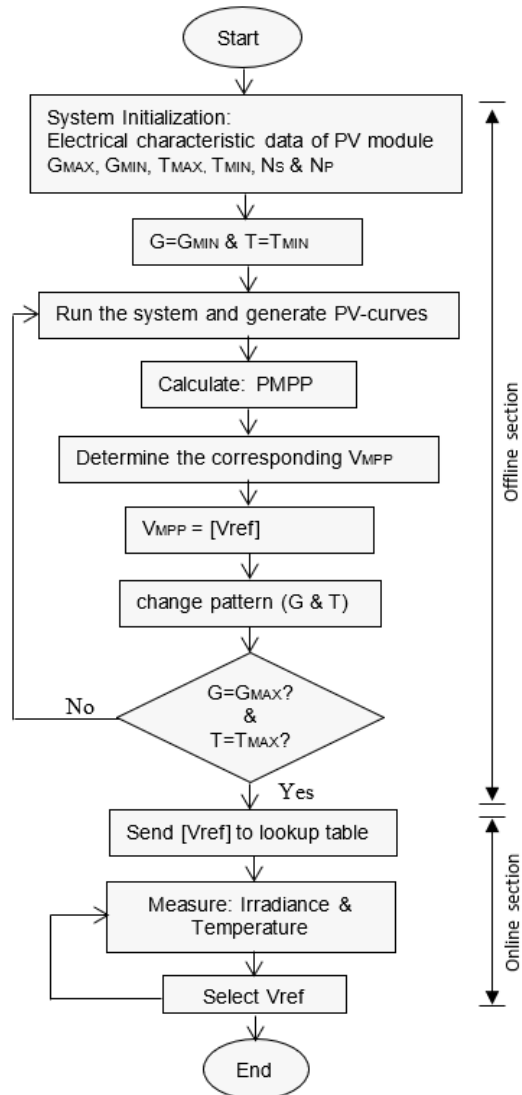


Fig. 3: The flowchart of the proposed algorithm.

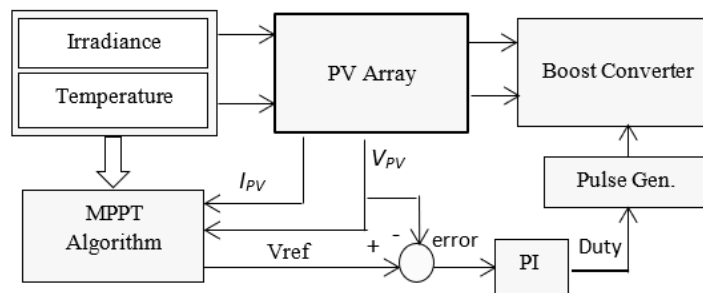


Fig. 4: The overall system with PI controller.

3.1 PV System Modeling under UICs and PSCs

Under UICs, the proposed method tests 400 patterns; 20 for changing solar irradiance (from 50 to 1000 W/m² by step change of 50 W/m²) x 20 for changing cell temperature (from 5 to 55 °C by step change of 5 °C). It runs the PV module for each pattern, measures the (V_{PV} , I_{PV} , and P_{PV}) and generates the PV curve for all these patterns, as shown in Fig. 5.

This method obtained the MPP for each pattern from the PV curves generated during the previous step, then calculates the corresponding reference voltage and sends it into an array. Figure 6 shows a 3-dimensional view of the array data, which contains a different irradiance, G and temperature, T as an input vector, and reference voltage (V_{ref}) as the output array.

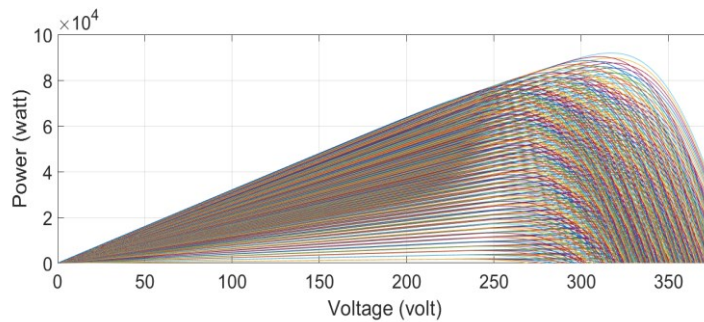


Fig. 5: The P-V curves for changing solar irradiance (50 to 1000 W/m²) and temperature (5 to 55 °C).

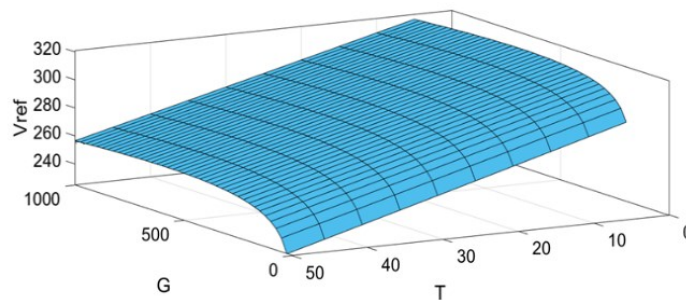


Fig. 6: The 3-dimensional view for irradiance (G), temperature (T), and reference voltage (V_{ref}) under UICs.

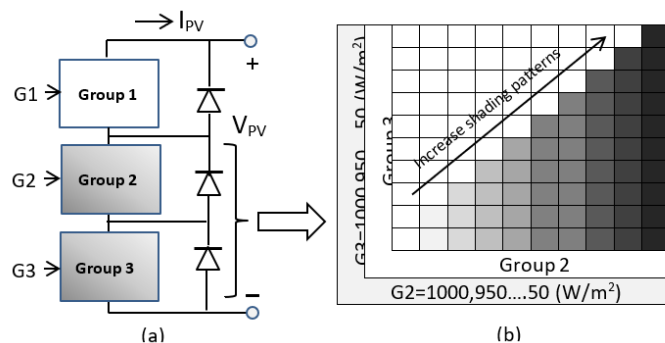


Fig. 7: Partially shaded PV array (a) three PV partial shading groups connected in series, (b) different shading patterns for two PV arrays.

Under PSCs, a PV module is shaded if three or more cells receive lower than the normal irradiance level [8,20]. Figure 7(a) shows the three groups of the PV module connected in series with 20 levels of different shading conditions for Groups 2 and 3. Under the partial

shading test, Group 1 is set as no shading PV array with 160 modules ((4-series) x (40-parallel)) and Groups 2 and 3 are shading PV arrays with 120 modules ((3-series) x (40-parallel)) for each. Figure 7(b) shows the different shading patterns (irradiance changed from 1000 to 50 W/m² for Group 2 and Group 3). The proposed algorithm was evaluated on 400 patterns (20x20), and the global maximum power point was calculated for each.

The P–V curves test obtained using the proposed method for a PV array with 400 modules (10×40) at a different shading pattern (one normal group and two shaded groups) is shown in Fig. 8. These curves are used to calculate the GMPP. From Fig. 8, notice that each PV-curve has one GMPP and one or more LMPP. It can also be seen that the only case in which the P-V curves contain one MPP is when all groups (Groups 1, 2, and 3) receive the same amount of irradiance.

From the obtained MPP, the proposed method calculates the voltage corresponding to the MPP for each pattern and considers it as a reference voltage (V_{ref}). To evaluate the system, we assumed that the system works under three different patterns; 1) pattern 104 ($G_1=1000$, $G_2=100$ and $G_3=300$ W/m²), 2) pattern 302 ($G_1=1000$, $G_2=100$ and $G_3=800$ W/m²) and 3) pattern 320 ($G_1=1000$, $G_2=1000$, and $G_3=800$ W/m²) where G_1 , G_2 , and G_3 are the amount of solar radiation falling on the groups (1, 2, and 3), respectively. These three patterns were chosen because each one gives a GMPP in a different location from the others. Fig. 9 shows a 3-dimensional view of different shading conditions for Groups 2 and 3, irradiance, and reference voltage for the PSCs test.

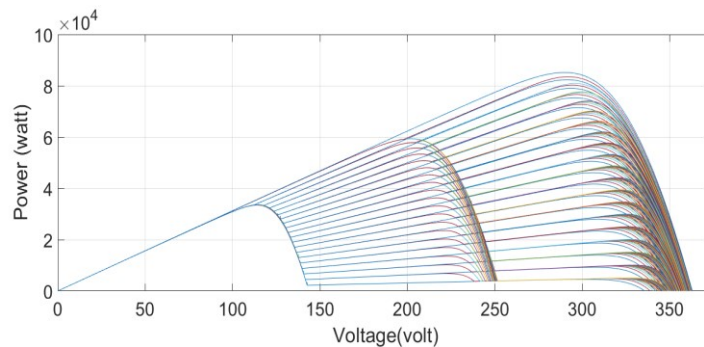


Fig. 8: PV curves testing of patterns 1 to 400 under PSCs.

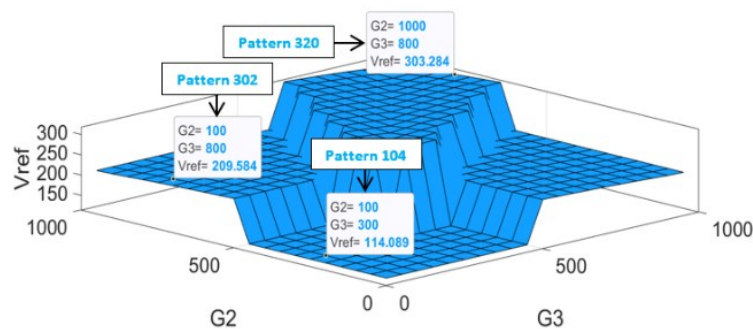


Fig. 9: The 3-dimensional view for irradiance and reference voltage under PSCs.

4. RESULTS AND DISCUSSION

Simulation analysis was conducted using MATLAB / SIMULINK and M-file code to verify the efficacy of the proposed method. This section analyses the proposed method's performance under uniform irradiance and partial shading conditions.

4.1 Uniform Irradiance Sudden Change

Figure 10 compares the dynamic response of the PV array output power (P_{PV}) based on the proposed and P&O methods under five-scenario uniform irradiance sudden changes (step increase on the left side and step decrease on the right side). Then, a comparison is made with the calculated MPPs as a reference signal calculated directly from the P-V curves. Fig. 10 shows that each MPPT technique (proposed and P&O) tracked the MPP for each step change. However, the proposed method reached the MPP with a faster speed response, greater accuracy, and lower steady-state fluctuations around the MPP compared with P&O MPPT at the same sudden changes in irradiance. The simulation results shown in Fig. 10 prove that the proposed method's effectiveness has been superior to the conventional P&O MPPT algorithm in terms of accuracy, tracking speed, and the fluctuations around the MPP. The reason is that it directly determines the optimum value of V_{ref} , taking it from the lookup table, which makes the proposed method very fast and accurate in reaching the MPP without a need to scan the voltage range on the P-V curve. Also, selecting one value of the V_{ref} caused the elimination of all fluctuations around the MPP.

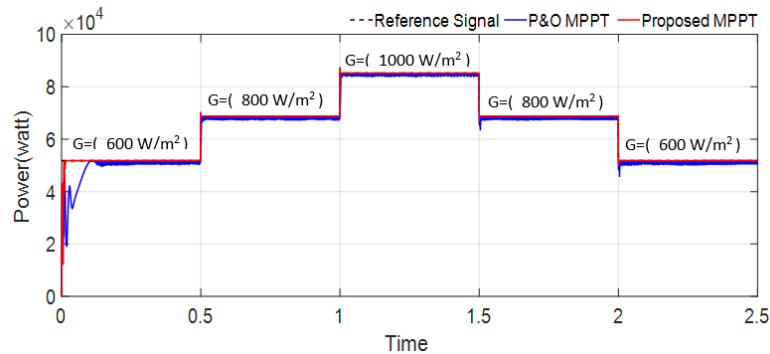


Fig. 10: Comparison of the output power of P&O and proposed MPPT techniques with the reference signal under sudden changes of irradiation.

Figure 11 shows the zoomed view of the output power during the first scanning process ($t = 0$ to 0.15 sec) and the sudden change in irradiance at $t = 1.5$ sec. From Fig. 11(a) and (b), the proposed method takes less time to reach the MPP than the conventional P&O algorithm. The time difference between them is $\Delta t = 0.133$ sec and $\Delta t = 0.04$ sec for the first scanning process at $t = 0$ sec and sudden change irradiance at $t = 1.5$ sec, respectively. This problem can be solved for the P&O algorithm by increasing the V_{ref} step size (ΔV_{ref}). Unfortunately, that would cause another problem, a more significant fluctuation around the MPP. As shown in Fig. 11, the proposed method reached the MPP with no power loss, while the P&O MPPT causes power losses ($\Delta P \approx 51800 - 51000 = 800$ watts) and ($\Delta P \approx 71817 - 68070 = 3737$ watts) for (a) and (b), respectively.

As mentioned before, the proposed method does not need a scanning process, making it very fast to reach the MPP. In the first scanning process shown in Fig. 11(a), the conventional P&O MPPT algorithm took a very long time to reach the MPP because it depends on the initial V_{ref} (in this case, V_{ref} initial equal to 250 volts), while the V_{MPP} equal to 293 volts at 600 W/m^2 . Another problem is that the P&O MPPT has very high fluctuations around the MPP compared to the proposed method, which has no fluctuations around the MPP. The fluctuations problem can be solved by decreasing the ΔV_{ref} . However, decreasing the ΔV_{ref} would slow down the output response. Also, it is evident from Fig. 11(b) that the maximum overshoot due to sudden change in irradiance is very small in the output power based on the proposed method. At the same time, it is higher for the conventional P&O

MPPT algorithm. The fluctuation and slow-down situations associated with the conventional algorithms cause additional power losses in the PV systems. These problems cannot be solved because both situations are related, so one needs to find an acceptable case between them.

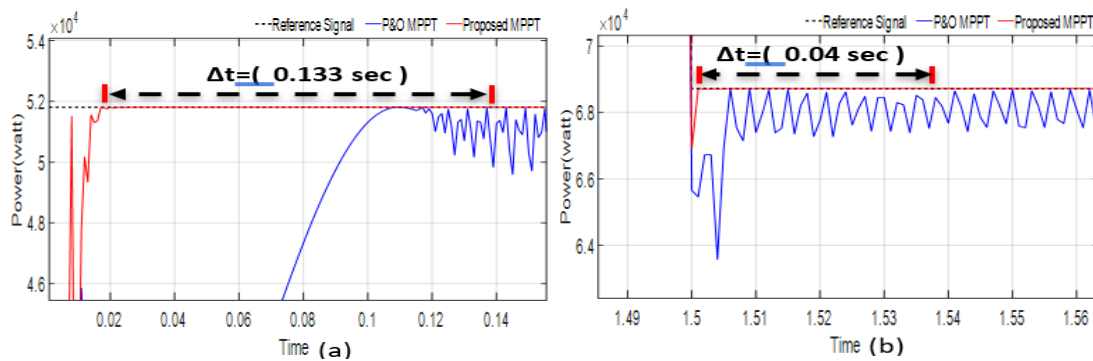


Fig. 11: Zoomed view of Fig. 10(a) due to the first scanning process (at $t = 0$ to 0.15 sec), (b) due to the sudden irradiance changes at ($t = 1.5$ sec).

4.2 Load Changes

This analysis is meant to verify the proposed method under hard conditions. The output resistance (R_{OUT}) of the boost converter is changed from 5Ω to 20Ω at ($t = 0.3$ sec) and then returned to 5Ω at ($t = 0.6$ sec) as shown in Fig. 12. It can be seen from Fig. 12 that the proposed method is superior by maintaining the dynamic response without fluctuations after the R_{OUT} has been changed. Further, when the load resistance disturbance occurred at $t = 0.3$ sec, the power losses reached approximately ($\Delta P \approx 85180 - 82600 = 2580$ watts) using the conventional P&O MPPT algorithm compared to the proposed method. At the same time, the P&O MPPT generates high fluctuations around the MPP at the steady-state response. Also, when the R_{OUT} return to 5Ω at $t = 0.6$ sec, the P&O MPPT takes about 0.11 sec to reduce the fluctuations and return the dynamic response to the first situation with power losses ($\Delta P \approx 85180 - 84200 = 980$ watts). The reason P&O MPPT was affected by changing the R_{OUT} is that the input resistance has been affected, which caused offsetting of the position of the operating point on the PV curve.

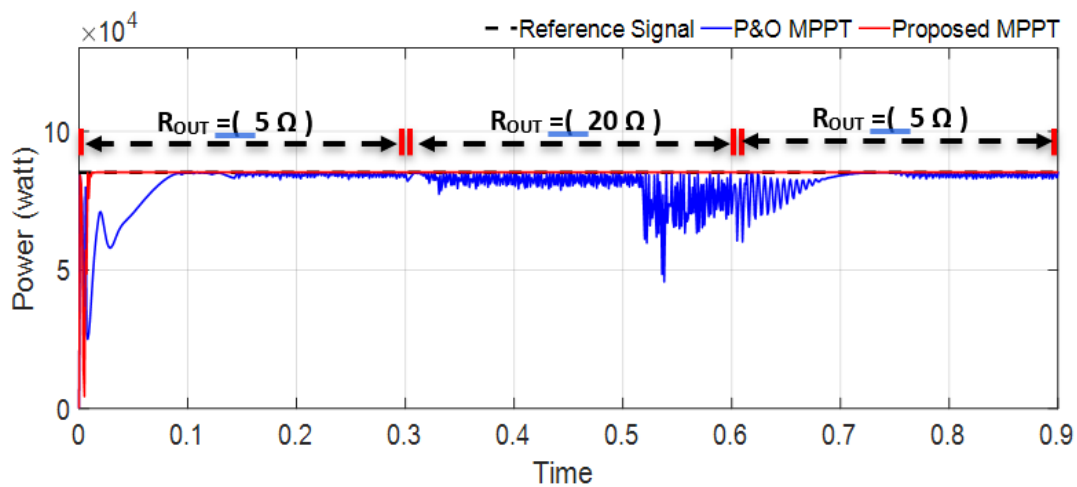


Fig. 12: Comparison of the output power of P&O and proposed MPPT techniques under load changes.

4.3 Partial Shading Conditions

This analysis aims to verify the proposed method’s ability to track GMPP under PSC. Three shading patterns have been generated where three PV module groups have been connected in series to simulate the partial shading conditions. The three patterns have three different shapes based on the location of the GMPP on the P-V curve, where each one has one GMPP. The GMPP for pattern 104 (point A) is located at the first peak, making it easy to track if the voltage range scan starts from zero, while for pattern 302 and pattern 320, the GMPPs are located at the second (point B) and third (point C) peak, respectively, which needs a unique tracking technique. Figure 13 shows the three different partial shading P-V curves for 1) pattern 104 ($G_1=1000$, $G_2=100$ and $G_3=300$ W/m^2), 2) pattern 302 ($G_1=1000$, $G_2=100$ and $G_3=800$ W/m^2) and 3) pattern 320 ($G_1=1000$, $G_2=1000$ and $G_3=800$ W/m^2).

It is observed that each P-V curve has 3 peaks, and the MPPT algorithm needs to scan all these peaks to decide which one represents the GMPP. Figure 13 shows the P-V curves of the sudden change scenario, assuming that a series of partial shading had just happened, which shifts the operating points from pattern 104 to pattern 302 to pattern 320 under PSCs at $t = 1$ and 1.5 sec, respectively. When partial shading scenarios occur, the P-V curves give multi LMPs and single GMPP for each pattern, where the goal here is to track the GMPP, which is point (A, B and C) in the shortest possible time.

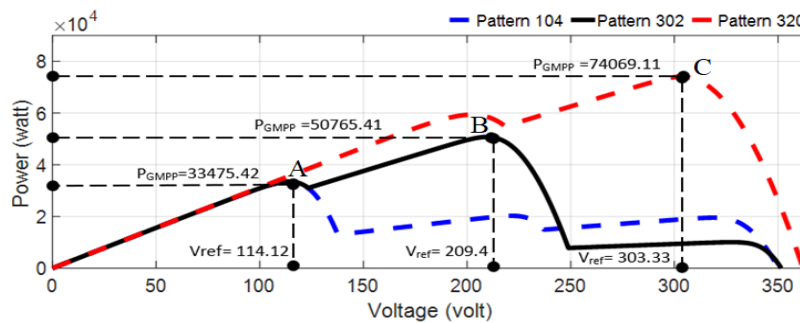


Fig. 13: Three different partial shading P-V curves for patterns 104, 302 and 320.

Figure 14 shows the PV output power response of the proposed method compared with the conventional P&O MPPT algorithm under PSCs, where the scenarios shown in Fig. 13 have been used. As seen in Fig. 14, both proposed, and conventional P&O MPPT has reached the GMPP at the first pattern (point A) at the first zone on the P-V curve. The P&O MPPT algorithm reached the GMPP because it is located in the first zone, making it easy to track based on the initial scanning voltage, which has been set in zone one. Even though the conventional MPPT algorithm tracked the GMPP, it took more time with very high fluctuations, while the proposed method reached the GMPP faster with fewer fluctuations around the GMPP ($\Delta t \approx 8$ msec).

At $t = 1$ sec, the operational point jumped from pattern 104 to pattern 302, which means that the GMPP has been moved to zone two on the P-V curve, point B. At this operational point, the conventional P&O MPPT algorithm could not track the GMPP because it is located on the second peak on the PV curve, while the start scanning point located within peak one depends on the first GMPP (point A). The conventional P&O MPPT algorithm will remain stuck in zone one when the scanning point crosses point A. The P&O MPPT algorithm would return due to low power indication. At this period, the P&O MPPT algorithm failed to track the GMPP, while the proposed method tracked the GMPP

accurately as fast as possible. The same process occurred when the operational point jumped to pattern 320.

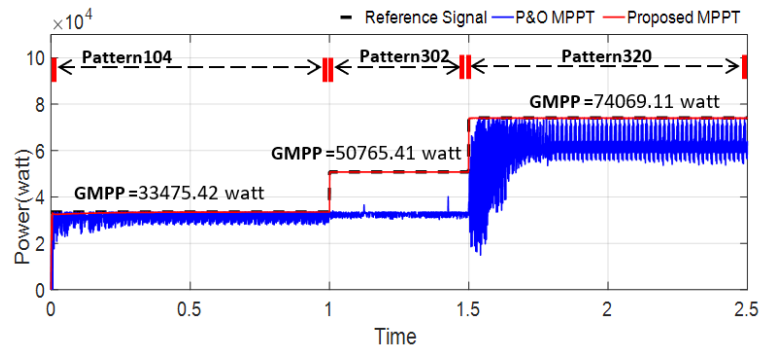


Fig. 14: Comparison of the output power of P&O and proposed MPPT techniques with the reference signal under PSCs with three different patterns.

In contrast, the proposed method reached the GMPPs of all three patterns in the shortest time without any fluctuations around the GMPP. The conventional MPPT algorithms fail to track the GMPPs under PSCs because they cannot jump from one zone to another on the P-V curve. At the same time, the proposed method was not affected by changing the operational point, which gives enough flexibility to move on the P-V curve.

Figure 15 shows the zoomed view of Fig. 14 for the three different patterns during the time intervals (0.1 to 0.16 sec), (1.1 to 1.25 sec), and (1.75 to 1.85 sec) for patterns 104, 302, and 320, respectively. It shows how the proposed method and the P&O MPPT algorithm tracked the GMPP when partial shading occurs. As shown in Fig. 15(a), the proposed method reached the GMPP during pattern 104 without any power loss, compared to the reference power signal, while the P&O MPPT tracked the GMPP but with power losses ($\Delta P = 33475.42 - 30745.45 = 2729.97$ watts). Also, the fluctuation around the GMPP is very high compared to the proposed method. The P&O MPPT algorithm can track the GMPP at this period because GMPP is located within the first peak. In the patterns 302 and 320 shown in Fig. 15(b) and Fig. 15(c), respectively, the P&O MPPT failed to track the GMPPs (50765.41 and 74069.11 watts) and instead tracked the first LMPP = 33493 watts for patterns 302 and second LMPP = 61499 watts for patterns 320, and missed tracking the GMPP because it did not locate in the second peak (pattern 302), or third peak (pattern 320). The overall simulation results substantiate that the proposed method's effectiveness has been superior to the conventional P&O MPPT algorithm in terms of accuracy, tracking speed, fluctuations around the MPP, and tracking the GMPP under PSCs.

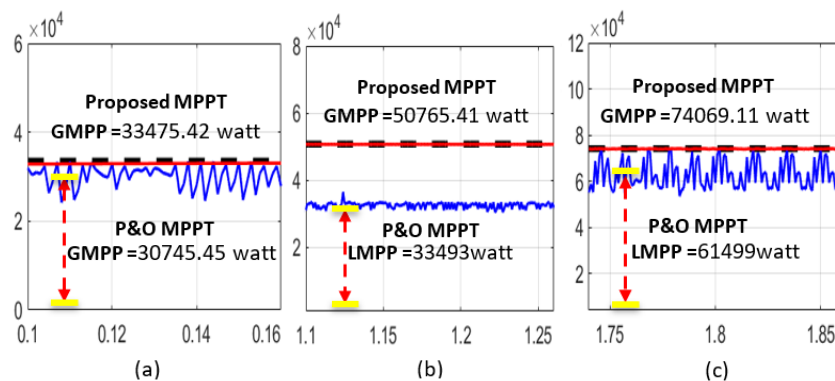


Fig. 15: Zoomed view of Fig. 14 (a) due to pattern 104, (b) due to pattern 302, (c) due to pattern 320.

5. CONCLUSION

This paper proposed an automatic and accurate method for tracking the MPP for any PV system under UICs and PSCs. It has fixed the complexity of determining the accurate lookup table data in an automatic and fast process under UICs and PSCs. The proposed method has been running the PV module with all potential irradiance and ambient temperatures to get the PV curve and then calculating the corresponding V_{MPP} automatically for each case. Then, the calculated array voltage was set as the PV array reference operating voltage [V_{ref}]. Five scenarios of sudden irradiance changes under UICs and three-pattern scenarios under PSCs were done to verify the proposed method. Compared with the conventional P&O MPPT technique, the proposed method harvests higher power from the PV system because it has a fast-tracking response, robust stability, and fewer fluctuations around the MPP. From the study, the lookup table data generated automatically using the proposed method worked ideally compared to conventional data collection methods. This method gives the lookup table control system the ability to track the GMPP under PSCs, which solves the weakness point associated with this kind of control system. A future recommendation to validate this method under all potential challenges is to test it with more extended string PV modules. This method will be the subsequent research investigation to be considered.

ACKNOWLEDGMENT

This research work is supported by the Ministry of Higher Education Malaysia for Fundamental Research Grant Scheme with Project Code: FRGS/1/2019/TK04/USM/02/12.

REFERENCES

- [1] Heelan MY, Al-Qrimli FAM. (2020) Design and simulation of neuro-fuzzy-based MPPT controller for PV power system. Proceedings of the Int. Conf. on Electrical, Communication, and Computer Engineering (ICECCE 2020), 12-13 June 2020, Istanbul, Turkey, pp. 1-6. doi: 10.1109/ICECCE49384.2020.9179287.
- [2] Zhang X, Gamage D, Wang B, Ukil A. (2021) Hybrid maximum power point tracking method based on iterative learning control and perturb & observe method. IEEE Trans. on Sustainable Energy, 12(1): 659-670. doi: 10.1109/TSTE.2020.3015255.
- [3] Ostadrahimi A, Mahmoud Y. (2021) Novel spline-MPPT technique for photovoltaic systems under uniform irradiance and partial shading conditions. IEEE Trans. on Sustainable Energy, 12(1): 524-532. doi: 10.1109/TSTE.2020.3009054.
- [4] Xu S, Gao Y, Zhou G, Mao G. (2021) A global maximum power point tracking algorithm for photovoltaic systems under partially shaded conditions using modified maximum power trapezium method. IEEE Trans. on Industrial Electronics, 68(1): 370-380. doi: 10.1109/TIE.2020.2965498.
- [5] Kumar N, Hussain I, Singh B, Panigrahi BK. (2018) Framework of maximum power extraction from solar PV panel using self-predictive perturb and observe algorithm. IEEE Trans. on Sustainable Energy, 9(2): 895-903. doi: 10.1109/TSTE.2017.2764266.
- [6] Bhattacharyya S, Kumar DSP, Samanta S, Mishra S. (2021) Steady output and fast tracking MPPT (SOFT-MPPT) for P&O and InC algorithms. IEEE Trans. on Sustainable Energy, 12(1): 293-302. doi: 10.1109/TSTE.2020.2991768.
- [7] Ahmed RM, Zakzouk NE, Abdelkader MI, Abdelsalam AK. (2021) Modified partial-shading-tolerant multi-input-single-output photovoltaic string converter. IEEE Access, 9: 30663-30676. doi: 10.1109/ACCESS.2021.3058695.
- [8] Hsieh G, Hsieh H, Tsai C, Wang C. (2013) Photovoltaic power-increment-aided incremental-conductance MPPT with two-phased tracking. IEEE Trans. on Power Electronics, 28(6): 2895-2911. doi: 10.1109/TPEL.2012.2227279.

- [9] Basoglu ME. (2019) Module level global maximum power point tracking strategy. Proceedings of the 2019 4th Int. Conf. on Power Electronics and their Applications (ICPEA), 25-27 Sept 2019, Elazig, Turkey, pp. 1-5. doi: 10.1109/ICPEA1.2019.8911173.
- [10] Gonzalez-Castano, Restrepo C, Kouro S, Rodriguez J. (2021) MPPT algorithm based on artificial bee colony for PV system. IEEE Access, 9: 43121-43133. doi: 10.1109/ACCESS.2021.3066281.
- [11] Zadeh MJZ, Fathi SH. (2017) A new approach for photovoltaic arrays modeling and maximum power point estimation in real operating conditions. IEEE Trans. on Industrial Electronics, 64(12): 9334-9343. doi: 10.1109/TIE.2017.2711571.
- [12] Reddy D, Ramasamy S. (2019) An artificial intelligent MPPT controller based three level SEPIC topology for 1.2kW solar PV system. Proceedings of the 2019 Innovations in Power and Advanced Computing Technology (i-PACT), 22-23 Mar 2019, Vellore, India, pp. 1-6. doi: 10.1109/i-PACT44901.2019.8960135.
- [13] Chandran A, Mathew BK. (2020) Comparative analysis of P&O and fuzzy logic controller based MPPT in a solar cell. Proceedings of the 2020 Third Int. Conf. on Smart Systems and Inventive Technology (ICSSIT), 20-22 Aug 2020, Tirunelveli, India, pp. 622-626. doi: 10.1109/ICSSIT48917.2020.9214187.
- [14] Udayalakshmi JK, Sheik MS. (2018) Comparative study of perturb & observe and lookup table maximum power point tracking techniques using MATLAB/Simulink. Proceedings of the 2018 Int. Conf. on Current Trends towards Converging Technologies (ICCTCT), 1-3 Mar 2018, Coimbatore, India, pp. 1-5. doi: 10.1109/ICCTCT.2018.8550835.
- [15] Rolevski M, Zecevic Z. (2020) MPPT controller based on the neural network model of the photovoltaic panel. Proceedings of the 24th Int. Conf. on Information Technology (IT), 18-22 Fen 2020, Zabljak, Montenegro, pp. 1-4. doi: 10.1109/IT48810.2020.9070299.
- [16] Bouazza F, Mohamed M, Bouziane B, Abdelhak D. (2019) Photovoltaic generator modeling based on lookup table approach and implementation on STM32F407 board of the perturb & observe algorithm based MPPT. Proceedings of the 2018 Int. Conf. on Applied Smart Systems (ICASS), 24-25 Nov 2018, Medea, Algeria, pp. 1-7. doi: 10.1109/ICASS.2018.8652000.
- [17] Ngo S, Chiu C. (2020) Simulation implementation of MPPT design under partial shading effect of PV panels. Proceedings of the 2020 Int. Conf. on System Science and Engineering (ICSSE), 31 Aug – 3 Sept 2020, Kagawa, Japan, pp. 1-6. doi: 10.1109/ICSSE50014.2020.9219306.
- [18] Alhussain HMA, Yasin N. (2020) Modeling and simulation of solar PV module for comparison of two MPPT algorithms (P&O & INC) in MATLAB/Simulink. Indonesian Journal of Electrical Engineering and Computer Science, 18(2): 666-677. doi: 10.11591/ijeecs.v18.i2.pp666-677.
- [19] Moreira HS, Gomes dos Reis MV, de Araujo LS, Perpetuo e Oliveira T, Villalva MG. (2017) An experimental comparative study of perturb and observe and incremental conductance MPPT techniques for two-stage photovoltaic inverter. Proceedings of the 2017 Brazilian Power Electronics Conference (COBEP), 19-22 Nov 2017, Juiz de Fora, Brazil, pp. 1-6. doi: 10.1109/COBEP.2017.8257370.
- [20] Ghasemi MA, Foroushani HM, Parniani M. (2016) Partial shading detection and smooth maximum power point tracking of PV arrays under PSC. IEEE Trans. on Power Electronics, 31(9): 6281-6292. doi: 10.1109/TPEL.2015.2504515.